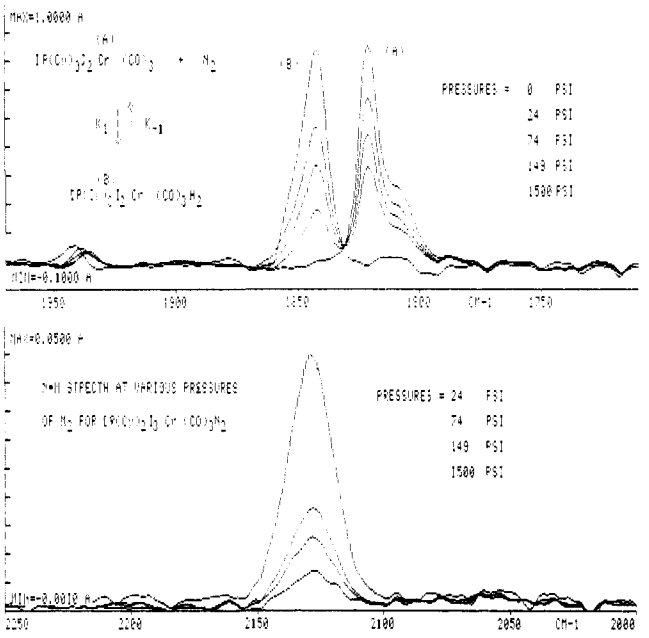

Figure 2. Infrared spectra of $(PCy_3)_2Cr(CO)_3$ under various pressures of N_2. The band at 1821 cm^{-1} due to $(PCy_3)_2Cr(CO)_3$ decreases as the band at 1843 cm^{-1} increases. The bottom figure shows the absorbance (scale expanded 20×) at 2128 cm^{-1} due to the N_2 stretch. Spectra run at 25.0 °C in toluene.

the order of 10 kcal/mol.[4b] Since the Cr-L bond is generally weaker than analogous Mo-L and W-L bonds, the hydrogen and nitrogen complexes fall below this and have net unfavorable free energies of formation. Either lowering the temperature or raising the pressure allows spectroscopic observation of the molecular hydrogen and nitrogen complexes. Infrared spectra of the reversible binding of hydrogen and nitrogen as a function of pressure are shown in Figures 1 and 2.

$$(PCy_3)_2Cr(CO)_3 + H_2 \rightleftharpoons (PCy_3)_2Cr(CO)_3(H_2) \quad (9)$$

$$(PCy_3)_2Cr(CO)_3 + N_2 \rightleftharpoons (PCy_3)_2Cr(CO)_3(N_2) \quad (10)$$

The chromium complex bears strong resemblence to the molybdenum and tungsten analogues; however, it also shows some important differences. Equilibrium data[6] indicate that it binds hydrogen more strongly than nitrogen, the opposite of behavior for the molybdenum and tungsten analogues. This is clearly shown in Figures 1 and 2 where higher pressures are needed to form the dinitrogen complex.

The preparation of this complex completes the series $(PCy_3)_2M(CO)_3$, M = Cr, Mo, W. There are few isolable complexes of this type known, and we are not aware of any which spans a complete triad of metals. This provides a good opportunity to investigate in detail the role of the metal in determining metal-ligand bond strengths in solution. Additional kinetic and thermodynamic studies on these and related complexes are in progress.

Acknowledgment. Support of this work by the National Science Foundation (Grant CHE-8618753) is gratefully acknowledged.

Registry No. $(PCy_3)_2Cr(CO)_3$, 114595-36-7; $(PCy_3)_2Cr(CO)_3(H_2)$, 114595-37-8; $(PCy_3)_2Cr(CO)_3(N_2)$, 114595-38-9; $(PCy_3)_2Cr(CO)_3(CH_3CN)$, 114595-39-0; $(PCy_3)_2Cr(CO)_3(py)$, 114595-40-3; $(PCy_3)_2Cr(CO)_3[P(OMe)_3]$, 114595-41-4; $(PCy_3)_2Cr(CO)_4$, 20957-94-2; $(PCy_3)_2Mo(CO)_3$, 73690-53-6; $(PCy_3)_2Mo(CO)_3(H_2)$, 104198-76-7; $(PCy_3)_2Mo(CO)_3(N_2)$, 73690-54-7; $(PCy_3)_2Mo(CO)_3(CH_3CN)$, 100995-28-6; $(PCy_3)_2Mo(CO)_3(py)$, 100995-30-0; $(PCy_3)_2Mo(CO)_3[P(OMe)_3]$, 114595-42-5; $(PCy_3)_2Mo(CO)_4$, 54873-46-0; $(PCy_3)_2W(CO)_3$, 73690-56-9; $(PCy_3)_2W(CO)_3(H_2)$, 104198-75-6; $(PCy_3)_2W(CO)_3(N_2)$, 73690-57-0; $(PCy_3)_2W(CO)_3(CH_3CN)$, 100995-29-7; $(PCy_3)_2W(CO)_3(py)$, 100995-31-1; $(PCy_3)_2W(CO)_3[P(OMe)_3]$, 100995-38-8; $(PCy_3)_2W(CO)_4$, 38800-78-1; $(C_7H_8)Cr(CO)_3$, 12125-72-3; $(C_{10}H_8)Cr(CO)_3$, 12110-37-1.

η^2-(N,C)-Pyridine and μ-η^2(1,2):η^2(4,5)-Benzene Complexes of (silox)$_3$Ta (silox = t-Bu_3SiO^-)

David R. Neithamer, László Párkányi,† John F. Mitchell, and Peter T. Wolczanski*‡

Department of Chemistry, Baker Laboratory Cornell University, Ithaca, New York 14853

Received February 5, 1988

The unusual capability of transition metals to coordinate to π-systems of organic molecules is recognized as playing a historic and important role in the growth of organometallic chemistry. This development is manifested in the widespread usage of aromatic hydrocarbons, such as cyclopentadienyl anion and arenes, as ancillary ligands bound with maximum hapticity to various metals.[1] Less common, but inherently interesting, are modes of binding which disturb the aromaticity of the fragment, yet fall short of utilizing the hydrocarbon's full complement of π-electrons.[1-7] Presented herein are pyridine (η^2)[7] and benzene $\{\mu$-$\eta^2(1,2)$:$\eta^2(4,5)\}$ adducts of $(silox)_3Ta$ (**1**, silox = t-Bu_3SiO^-)[8] which exhibit intriguing coordination geometries.

Treatment of pale blue **1** with pyridine, 1.0 equiv or an excess, resulted in the formation of an orange solution from which amber crystals of $(silox)_3Ta\{\eta^2$-(N,C)-$NC_5H_5\}$ (**2**) could be isolated in 65% yield (Figure 1). ^1H and ^{13}C NMR spectra of **2** revealed 5 inequivalent ring positions, including a broad singlet at δ 3.89 and corresponding α-carbon resonance at δ 81.96. Table I lists the spectral assignments of **2** as determined via comparisons with the free ligand,[9] decoupling, HETCOR, and labeling studies. An X-ray structural investigation of the complex[10] fully established the η^2 coordination mode of the pyridine.[7,11,12] The skeletal view

† On leave from the Central Research Institute of Chemistry, Hungarian Academy of Science, Budapest, Hungary.

‡ Alfred P. Sloan Foundation Fellow (1987-1989).

(1) (a) Collman, J. P.; Hegedus, L. S.; Norton, J. R.; Finke, R. G. *Principles and Applications of Organotransition Metal Chemistry*; University Science Books: Mill Valley, CA, 1987. (b) Yamamoto, A. *Organotransition Metal Chemistry*; John Wiley and Sons: New York, 1986.

(2) (a) Muetterties, E. L.; Bleeke, J. R.; Wucherer, E. J.; Albright, T. A. *Chem. Rev.* **1982**, *82*, 499-525. (b) Jonas, K. *Angew. Chem., Int. Ed. Engl.* **1985**, *24*, 295-311.

(3) (a) Jones, W. D.; Feher, F. J. *J. Am. Chem. Soc.* **1984**, *106*, 1650-1663. (b) Jones, W. D.; Feher, F. J. *Ibid.* **1986**, *108*, 4814-4819. The latter article contains a pertinent discussion of isotope effects pertaining to η^2-arenes.

(4) (a) Sweet, J. R.; Graham, W. A. G. *J. Am. Chem. Soc.* **1983**, *105*, 305-306. (b) Sweet, J. R.; Graham, W. A. G. *Organometallics* **1983**, *2*, 135-140. (c) Brauer, D. J.; Kruger, C. *Inorg. Chem.* **1977**, *16*, 884-891. (d) Jonas, K. *J. Organomet. Chem.* **1974**, *78*, 273-279. (e) Werner, H.; Gotzig, J. *Ibid.* **1985**, *284*, 73-93.

(5) (a) Harman, W. D.; Taube, H. *J. Am. Chem. Soc.* **1987**, *109*, 1883-1885. (b) van der Heijden, H.; Orpen, A. G.; Pasman, P. *J. Chem. Soc., Chem. Commun.* **1985**, 1576-1578.

(6) Bruck, M. A.; Copenhaver, A. S.; Wigley, D. E. *J. Am Chem. Soc.* **1987**, *109*, 6525-6527, and references therein.

(7) Evidence for $[(H_3N)_5Os\{\eta^2$-(C,C)-lutidine$\}]^{2+}$ has recently been obtained: Cordone, R.; Taube, H. *J. Am. Chem. Soc.* **1987**, *109*, 8101-8102.

(8) LaPointe, R. E.; Wolczanski, P. T.; Mitchell, J. F. *J. Am. Chem. Soc.* **1986**, *108*, 6382-6384.

(9) Katritsky, A. R.; Rees, C. W.; Boulton, A. J.; McKillop, A. *Comprehensive Heterocyclic Chemistry*; Pergamon Press: New York, 1984; Vol. 2, pp 1-28. J_{CH} for py: C_α, 178; C_β, 162; C_γ, 162 Hz. Bond lengths for py: N-C_α (1.338 Å), C_α-C_β (1.394 Å), C_β-C_γ (1.392 Å).

(10) Crystal data for $(silox)_3Ta\{\eta^2$-(N,C)-$NC_5H_5\}$ (**2**): orthorhombic, *Pbca*, λ(Cu Kα), μ = 51.87 cm^{-1}, a = 22.378 (12) Å, b = 32.582 (13) Å, c = 13.162 (4) Å, T = 25 °C, Z = 8, V = 9596.2 (72) Å^3, R = 0.051, R_w = 0.075, 5340 (82.5%) reflections where $|F_o| \geq 1.5\sigma(F_o)$. Other angles: N-C1-C2, 120.4 (11)°; C1-C2-C3, 118.6 (12)°; C2-C3-C4, 124.8 (12)°; C3-C4-C5, 119.8 (13)°; C4-C5-N, 112.5 (11)°; Ta-C5-N, 69.1 (6)°; Ta-N-C5, 70.2 (6)°; C5-Ta-N 40.7 (5)°; C5-Ta-O1,O2,O3, 117.4 (4), 119.5 (5), 93.4 (4)°; N-Ta-O1,O2,O3, 101.9 (4), 96.8 (3), 133.6 (3)°. Esd's for the (silox)$_3$Ta core: Ta-O, 0.006 Å; Si-O, 0.007 Å; ∠Ta-O-Si, 0.4°.

(11) For similar bound imine complexes, see: Mayer, J. M.; Curtis, C. J.; Bercaw, J. E. *J. Am. Chem. Soc.* **1983**, *105*, 2651-2660, and references therein.

(12) For η^6-py complexes, see: (a) Morris, R. H.; Ressner, J. M. *J. Chem. Soc., Chem. Commun.* **1983**, 909-910. (b) Timms, P. L. *Angew. Chem., Int. Ed. Engl.* **1975**, *14*, 273-277. (c) Choi, H. W.; Sollberger, M. S. *J. Organomet. Chem.* **1983**, *243*, C39-C41. (d) Simons, L. H.; Riley, P. E.; Davis, R. E.; Lagowski, J. J. *J. Am. Chem. Soc.* **1976**, *98*, 1044-1045.

0002-7863/88/1510-4421$01.50/0

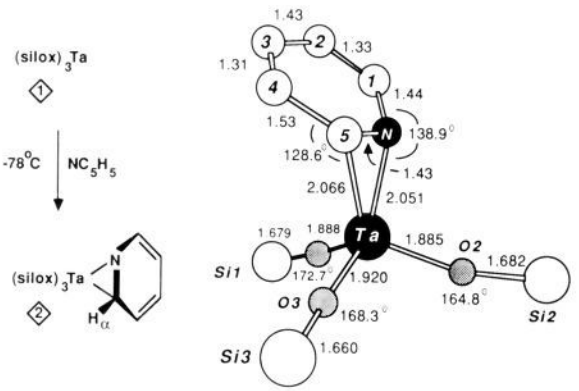

Figure 1.

Table I. ^{1}H and ^{13}C NMR Spectra of (silox)$_3$Ta{η^2(N,C)-NC$_5$H$_5$} (2)

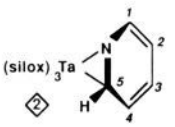

assnmt	δ(^{1}H, C_7D_8)	$J_{HH'}$ (±0.2 Hz)	δ(^{13}C, C_6D_{12})	$^1J_{CH}$ (Hz)
CH(1)	7.40, d"m"	$^3J_{1,2}$ = 6.2	144.75, d	175
CH(2)	5.22, "t"	$^3J_{1,2}$ = 6.2, $^3J_{2,3}$ = 5.7	109.69, d	160
CH(3)	5.73, dddd	$^3J_{3,4}$ = 9.3, $^3J_{2,3}$ = 5.7, J = 1.7, 1.0	121.30, d	158
CH(4)	6.44, d"t"d	$^3J_{3,4}$ = 9.3, J = 1.6, <0.5	128.24, d	158
CH(5)	3.89, br s		81.96, d	157
silox	1.21, s		31.05, q 23.94, s	125

in Figure 1 illustrates the pseudotetrahedral geometry of **2** (109 (3)° av), highlighting the rough 3,5-diene geometry of the ligand. Both C1–C2 (1.328 (16) Å) and C3–C4 (1.312 (22) Å) exhibit double bond distances, while an elongated C4–C5 (1.530 (19) Å) and intermediate C2–C3 (1.430 (18) Å), N–C1 (1.443 (16) Å) and C5–N (1.431 (17) Å) bond lengths are found.[9] Rather short Ta–C5 (2.066 (11) Å) and Ta–N (2.051 (11) Å) bond distances are observed, the latter perhaps indicative of minimal N π-donation, given the greater 138.6 (12)° Ta–N–C1 angle as compared to Ta–C5–C4 (129.2 (15)°). The structure is indicative of a Ta(V) complex, requiring an interruption of the pyridine π-system, thus corroborating the metallaaziridine depiction. The η^2-binding mode forces the α-H proximate to Ta, probably within 2.2 Å, but an agostic interaction has not been evidenced by IR. Proton–proton coupling to H5 is diminished, consistent with its distortion out of the NC_5H_5 plane, and the $J_{CH(5)}$ of 157 Hz is correspondingly 20–25 Hz lower than typical Cα ($J_{CH(1)}$ = 175 Hz) values.[9] Furthermore, **2**-d_1, prepared from α-D-pyridine, contained 50 (3)% D at the H1 and H5 positions (^{1}H, ^{2}H NMR); hence, no equilibrium isotope effect[3,13] was observed.

Upon standing for 10–14 days in benzene, a concentrated solution (~0.05 M) of (silox)$_3$Ta (**1**) deposited dark brown crystals of [(silox)$_3$Ta]$_2${μ-η^2(1,2):η^2(4,5)-C$_6$H$_6$} (**3**, ~7%) while cyclometallating to (silox)$_2$HTaOSi(t-Bu)$_2$CMe$_2$CH$_2$ (**4**, Figure 2).[8] An X-ray structure determination proved necessary,[14] since the complex was virtually insoluble in hydrocarbon and ethereal solvents. Figure 2 exhibits the pseudotetrahedral Ta centers (109 (6)° average) of **3**·2C$_6$H$_6$, revealing the inversion center amid the benzene ring and indicating a rough alignment of the Ta–C37–C38

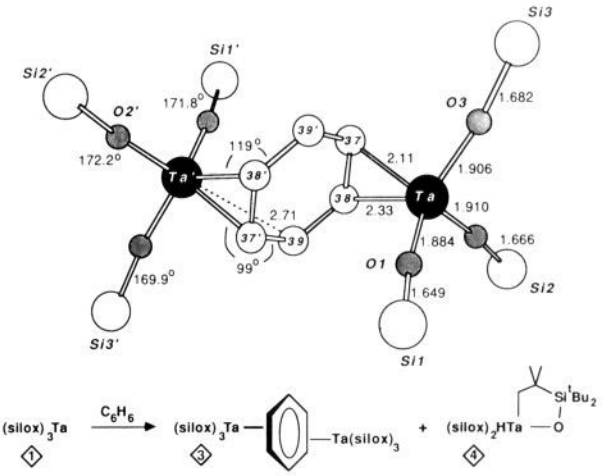

Figure 2.

plane with the Ta–O3 bond. Sterics dominate the orientation around the benzene, the bulky silox groups engender the trans 1,2:4,5 arrangement rather than the precedented trans 1,2:3,4,[5] and the six silox ligands pack in a staggered configuration about the Ta$_2$(μ-C$_6$H$_6$) unit. Differing Ta–C bonds (2.11 (1) and 2.33 (1) Å) support asymmetric binding to the arene, and the dihedral angle between the Ta–C37–C38 and benzene planes is severe (108°). Although the latter might suggest that **3** is a clathrate compound, the Ta–C bond lengths[15] are conclusive proof of a significant bond. A corresponding elongation of C37–C38 is expected, but the geometry of the μ-benzene fragment could not be accurately determined.[14] In this context it must be noted that Ta–C39′ is only 2.71 (1) Å, thus a bis-allyl depiction cannot be wholly discounted.[16] The C_i symmetry of the benzene renders **3** diamagnetic, as confirmed via magnetic measurements (Faraday balance).

The substantial reducing power and steric properties of (silox)$_3$Ta (**1**)[8] are clearly manifested in the unusual binding modes found for both pyridine and benzene. In coordinating to these aromatics in an η^2 fashion, the Ta can achieve its highest formal oxidation state. The unobserved N-bound pyridine-adduct may be electronically unfavorable due to a 4-e$^-$ repulsion between the filled d_{z^2} orbital of **1** and the N lone pair, provided $d\pi \rightarrow p\pi^*$ backbonding to NC_5H_5, considered a weak π-acid, is minimal. In the η^2-form, the latter type of interaction is maximized to the extent that the Ta–C and Ta–N bonds appear to be σ in character. Transients containing related η^2-(N,C)-pyridine moieties may be present prior to reported Cα activations[17,18] and during η^2-(C,C)

(13) (a) Wolfsberg, M. *Acc. Chem. Res.* **1972**, *5*, 225–233. (b) Clawson, L.; Soto, J.; Buchwald, S. L.; Steigerwald, M. L.; Grubbs, R. H. *J. Am. Chem. Soc.* **1985**, *107*, 3377–3378. (c) Calvert, R. B.; Shapley, J. R. *Ibid.* **1978**, *100*, 7726–7727. (d) Calvert, R. B.; Shapley, J. R.; Schultz, A. J.; Williams, J. M.; Suib, S. L.; Stucky, G. D. *Ibid.* **1978**, *100*, 6240–6241.

(14) Crystal data for [(silox)$_3$Ta]$_2${μ-η^2(1,2):η^2(4,5)-C$_6$H$_6$}·2C$_6$H$_6$ (**3**·2C$_6$H$_6$): triclinic, $P\bar{1}$, λ(Mo Kα), μ = 23.24 cm^{-1}, a = 13.200 (2) Å, b = 16.734 (2) Å, c = 12.655 (3) Å, α = 102.51 (1)°, β = 116.21 (2)°, γ = 83.54 (2)°, T = 25 °C, Z = 2, V = 2447.9 Å^3, R = 0.042, R_w = 0.064, 4291 (99.5%) reflections where $|F_o| \geq 3\sigma(F_o)$. The bound and solvent benzenes were poorly resolved (C–C bond lengths ranged from 1.30–1.45 Å and C–C–C angles from 110–130°, each with large esd's), hence a model including constraints (C–C 1.400 ± 0.006 Å; ∠C–C–C = 120 ± 1°) was applied via the program CRYSTALS. The esd's of the restrained distances and angles were used as "observational" weights in the normal equations; virtually no change in R was noted. Attempts to describe **3** through various disordered models and alternate arrangements resulted in no improvement. Final constrained distances and angles: C37–C38, 1.419 (9) Å; C37–C39′, 1.403 (10) Å; C38–C39, 1.400 (11) Å; ∠C38–C37–C39, 116.9 (12)°; ∠C37–C38–C39, 124.4 (12)°; ∠C38–C39–C37′, 117.6 (12)°. Other angles: C37–Ta–O1,O2,O3, 121.1 (3), 111.1 (3), 95.3 (3)°; C38–Ta–O1,O2,O3, 110.6 (3), 86.0 (2), 129.1 (3)°. Esd's for the (silox)$_3$Ta core: Ta–O, 0.006 Å; Si–O, 0.006 Å; ∠Ta–O–Si, 0.4°.

(15) (a) La Pointe, R. E.; Wolczanski, P. T.; Van Duyne, G. D. *Organometallics* **1985**, *4*, 1810–1818. (b) Schultz, A. J.; Brown, R. K.; Williams, J. M.; Schrock, R. R. *J. Am. Chem. Soc.* **1981**, *103*, 169–176, and references therein.

(16) Koepe, G.; Schieferstein, L.; Mynott, R.; Krüger, C.; Tsay, Y.-H.; Jonas, K. *Angew. Chem., Int. Ed. Engl.* **1983**, *22*, 620–621.

(17) For pyridyl complexes, see: (a) Klei, E.; Teuben, J. H. *J. Organomet. Chem.* **1981**, *214*, 53–58. (b) Watson, P. L. *J. Chem. Soc., Chem. Commun.* **1983**, 276–277. (c) Thompson, M. E.; Baxter, S. M.; Bulls, A. R.; Burger, B. J.; Nolan, M. C.; Santarsiero, B. D.; Schaefer, W. P.; Bercaw, J. E. *J. Am. Chem. Soc.* **1987**, *109*, 203–219.

to N-donor rearrangements.[7] Although it is difficult to assess how much of the resonance stabilization energy attributed to both NC_5H_5 and C_6H_6 (~35 Kcal/mol)[19] is lost upon coordination, σ-bonding to Ta must provide compensation. With pyridine, formation of a strong Ta-N bond may be critical, whereas η^2-bonding to two Ta centers is needed for benzene complexation. No mono-C_6H_6 adducts, $\eta^{2\,1-4,6}$ or $\eta^{4,1,5}$ have been observed in the course of these studies. Investigations of $(silox)_3Ta$ adduct formation and theoretical inquiries into the electronic natures of **1**, **2**, and **3** are ongoing.

Acknowledgment. Support from the Air Force Office of Scientific Research, the National Science Foundation (CHE-8714146), and Cornell University is gratefully acknowledged. We thank Darrin Richeson for Faraday measurements.

Supplementary Material Available: Tables of crystal data, fractional coordinates, isotropic and anisotropic thermal parameters, bond distances, and bond angles and experimental information pertaining to the X-ray crystallographic studies of **2** and **3**·$2C_6H_6$ (16 pages); tables of observed and calculated structure factors (45 pages). Ordering information is given on any current masthead page.

(18) (a) Fanwick, P. E.; Kobriger, L. M.; McMullen, A. K.; Rothwell, I. P. *J. Am. Chem. Soc.* **1986**, *108*, 8095-8097. (b) Erker, G.; Muhlenbernd, T.; Benn, R.; Rufinska, A. *Organometallics* **1986**, *5*, 402-404.

(19) (a) Benson, S. W. *Thermochemical Kinetics*; John Wiley and Sons: New York, 1968. (b) George, P. *Chem. Rev.* **1975**, *75*, 85-112.

Time Domain Spectroscopic Studies of Mixed-Valent Perovskites

Russell S. Drago,* Peter E. Doan, and Michael K. Kroeger

Department of Chemistry, University of Florida Gainesville, Florida 32611

Received March 10, 1988

We would like to report the measurement of rates of dielectric relaxation related to electron hopping in a set of mixed-valence strontium doped lanthanum orthoferrites $La_{1-x}Sr_xFeO_3$ by using Time Domain Spectroscopy (TDS). Introducing a Sr^{2+} defect into the lattices to balance the charge leads to an Fe(IV) site in the Fe(III) lattice. Early work by Gallagher and MacChesney[1] and Shimony and Knutson[2] using ^{57}Fe Mossbauer shows that the Fe sites have isomer shifts which suggest averaged oxidation states at room temperature and locked valence at 77 K. Further work by Takano et al.[3] show the isomer shifts vary with dopant level in a fashion that is consistent with averaged sites. Because the time scales associated with our TDS apparatus are at least 2 orders of magnitude faster than the ^{57}Fe Mossbauer experiment, we decided to investigate the dielectric relaxation in the neighborhood of room temperature.

The spectra obtained show a very strong dielectric relaxation in the doped systems that is not present in the undoped material. There is also measurable conductance in each of the doped samples. Highly conducting samples create problems in the interpretation of dielectric measurements by creating an effective relaxation time, τ, related to the magnitude of the static dielectric constant of the medium and the DC conductance,[4] σ. In general, TDS can measure the ohmic conductivity of the sample, but due to geometry and sample contact problems, the values obtained will only be relative, However, if the sample geometry remains relatively constant throughout the temperature range, the value obtained for the activation energy should be accurate.

Table I. Dielectric, Conductivity, and Relaxation Results

T (K)	τ (ps)	$\sigma \times 10^6$ (mho/cm)	dielectric loss $\epsilon_s - \epsilon_\infty$
	0.1 Sr^{2+} Doped		
334	1171 (30)	284 (32)	50.8
332	1346 (33)	211 (28)	51.4
310	1570 (36)	140 (25)	52.8
298	1801 (37)	105 (23)	52.0
283	2303 (63)	87 (22)	47.9
259	2813 (68)	52 (21)	41.3
	0.2 Sr^{2+} Doped		
335	1963 (46)	647 (45)	61.2
323	1813 (30)	574 (46)	53.6
312	2190 (44)	465 (37)	51.2
297	2028 (43)	394 (35)	44.1
283	2086 (57)	289 (29)	36.9
259	2194 (80)	202 (27)	30.6
	0.3 Sr^{2+} Doped		
340	1476 (31)	523 (35)	55.7
321	1464 (33)	484 (33)	50.1
297	1577 (35)	403 (30)	43.8
283	1634 (45)	334 (28)	37.0
259	1668 (28)	257 (26)	29.3

[a] The values in parentheses represent the standard deviations.

The dielectric relaxation times,[5] loss values for that relaxation, and DC conductivities for the sample with $X = 0.1$, 0.2, and 0.3 are shown in Table I. Other relaxation effects appear at very short times (up to 1 ns after the pulse), but our present analysis cannot adequately measure these rates because the Guggenheim plots are strongly curved, which suggests a distribution of relaxation times. In all three systems, the temperature behavior of the loss $(\epsilon_s - \epsilon_\infty)$ related to this relaxation shows a strong increase in magnitude with increasing temperature. This is related to the number of mobile charges in the lattice and shows there is some type of thermal "trapping" occurring at the lower temperatures.

The values obtained for the barriers to conductance (0.178, 0.119, and 0.067 eV for $X = 0.1$, 0.2, and 0.3 Sr(II) doping, respectively) and dielectric relaxation (0.082, 0.014, and 0.019 eV for 0.1, 0.2, and 0.3 Sr(II) doped) show the barrier to conductance is substantially higher than that for relaxation in all three systems. This corresponds to the expected trends for these systems. The mechanism for dielectric relaxation involves electron hopping near the defect; the distance between the positive and negative centers does not change. Conduction in these compounds takes place through electron diffusion between defect sites. The activation barrier would depend upon the distance between sites. The barriers fit the expected trend where $\Delta E_{(\text{conductance})}$ is greater than $\Delta E_{(\text{relaxation})}$.

(1) Gallagher, P. K.; MacChesney, J. B. *Symp. the Faraday Soc.* **1968**, *1*, 40.

(2) Shimony, U.; Knudsen, J. M. *Phys. Rev.* **1966**, *144*, 361.

(3) Takano, M.; Kawachi, J.; Nakanishi, N.; Takeda, Y. *J. Solid State Chem.* **1981**, *39*, 75.

(4) The experimental frequency (ω) dependent dielectric constant $\epsilon\times(\omega)$ is given by

$$\epsilon^*(\omega) = \epsilon'(\omega) - i\epsilon''(\omega) + [\sigma/i\omega\epsilon_0]$$

where $\epsilon'(\omega)$ is the real dielectric contribution; $i\epsilon''(\omega)$, the imaginary; the term containing σ (the DC conductivity) is the ohmic contribution, and ϵ_0 is the permittivity of free space. According to the Debye Model

$$\epsilon'(\omega) - i\epsilon''(\omega) = \epsilon_\infty + [(\epsilon_s - \epsilon_\infty)/(1 + i\omega\tau)]$$

where ϵ_s is the static dielectric constant and ϵ_∞ is the instantaneous dielectric constant. This lumps all relaxation effects due to conductivity ($\tau^{-1} = \sigma/\epsilon_0\epsilon$) into dielectric loss. There is no way using dielectric measurements alone to separate these effects. See: Cole, R. H.; Windsor, P. *Fourier Transform Dielectric Spectroscopy*; Plenum Press: New York, 1982.

(5) The rate of dielectric relaxation is not the same as the rate of electron transfer. However, to correct for the difference requires knowledge of the high and low frequency dielectric constants to a degree we cannot obtain with these systems.

0002-7863/88/1510-4423$01.50/0